

# Finite element code for modal analysis on navigation locks considering fluid structure interaction

João V. S. T. Araújo<sup>1</sup>, P. M. V. Ribeiro<sup>1</sup>

<sup>1</sup>*Dept. of Civil and Environmental Engineering, Federal University of Pernambuco  
Rua Acadêmico Hélio Ramos, 50740-530, Recife, Brazil  
soaresvictorjoao@gmail.com, paulo.vribeiro@ufpe.br*

**Abstract.** Navigation locks are classified as hydraulic structures inside the engineering domain and represent huge importance for the waterways system, once they turn the waterbodies navigable by enabling the ships to overcome unevenness. Through a mechanical point of view, this type of structure reunites two distinct types of materials: one solid, the other fluid. From the contact between those two fields, the fluid-structure interaction arises, characterized by pressure and deformation compatibility, due to dynamic coupling. Whether before the variety of the studied cases were limited by extensive analytical solutions and simplified geometry, at the last fifty years, due to the evolution of numerical methods, there was an advancement on the diversity of possible cases to be assessed over conditions closer to the reality concerning the geometry. Therefore, the present paper proposes the study of bidimensional cases of reinforced concrete navigation locks based on a unique MATLAB finite element method code. The cases will be submitted to modal analysis and their results will be validated on the ANSYS software. Those analyses will allow the identification of intervenient parameters on the structure behavior. From the outcomes interpretation, solutions will be formulated towards a design of those structures more consistent and less vulnerable to this type of solicitation.

**Keywords:** Navigation Locks, Fluid Structure Interaction, Finite Element Method, Modal Analysis.

## 1 Introduction

Navigation locks are robust structures that compound waterborne systems and their main use is to make waters navigable due to their ability to surpass the unevenness between two fluid bodies. Regarding the cargo sector, inland navigation emerges as a feasible alternative to road transportation, since the latter, despite its market dominance, begins to show signs of exhaustion. In this perspective, navigation locks are key elements for the branch of logistic goods by presenting interesting ecological and economic characteristics.

The primary approach to this subject, that involves fluids and structures, evaluates the hydrodynamics pressure development in rigid wall dams (Westergaard [1]). Afterward, Housner [2] performed a new analysis in which a division on the hydrodynamics pressure was made and classified as convective and impulsive pressures. This progress was relevant to start to appear in a great number of international design codes at that time. Structures framed in this kind of problem once were represented by monolithic blocks, but this simplification isn't made anymore. Nowadays they are considered flexible of elastic and inelastic proprieties, and as a result, there is a significant change in their dynamic response (Reitherman [3]). The fluid-structure interaction (FSI) materializes the dynamic coupling between these two entities, and by that, displacements and pressures domains require a simultaneous solution of their governing equations. The multiples intervenients variables in this kind of interaction exemplify the complex character of this problem, namely: geometry and structure flexibility (Rezaiee-Pajand [4]), water depths (Ma [5]), fluid compressibility (Xing [6]), and cavity width (Miquel [7]). In face of what was described, a thorough and systematic approach during the design process is primordial to prevent a potential collapse of this kind of structure avoiding catastrophic consequences (Mendes [8]).

The present work develops a unique code, implemented on MATLAB software, and validated by an ANSYS application. This script is dedicated to the assessment of modal response considering the FSI in locks, yet unpublished on the national scenario. Two distinct cases are exposed to evaluate parameters as water depths, cavity width, and structure dimension. By doing so, authors expect to contribute with an evolution towards a major concern on the design and serviceability maintenance during an external excitation.

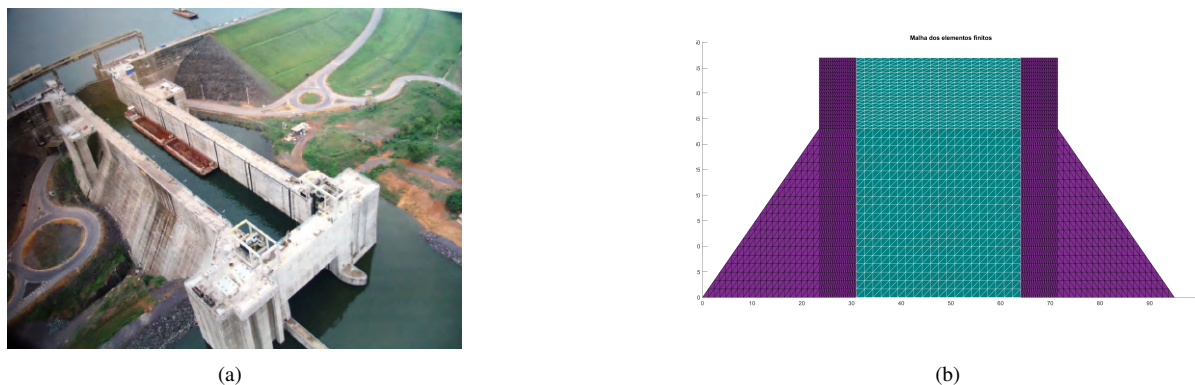


Figure 1. (a): Aerial view of Tucuruí's navigation lock. Transportation [9]; (b): Sample FEM mesh from the authors' code.

## 2 Theoretical formulation

### 2.1 Establishment of governing equations and finite elements approach

As exposed previously, hydraulic structures embrace two distinct natures, and to perform subsequent analyses, knowing its respective mathematical formulations is paramount. To simplify, some initial hypotheses are assumed in an effort to make numerical procedures feasible, but at the same time, be able to present support in a real case. The solid will be considered as an elastic linear isotropic material. The transversal dimension is considerably larger when compared to the longitudinal lock section, in a way that the assumption of a plane strain behavior is appropriated. The governing equations to this domain, are derived by the bidimensional theory of elasticity. Fig2b displays the considered variables of the eq. (1a) by implying the equilibrium of the infinitesimal element, where  $\sigma$  represents the normal stresses,  $\tau$  is for shear stress,  $f$  for body force and  $c$  gives the sonic velocity in fluid domain.

The fluid is assumed acoustic, homogeneous, inviscid, incompressible, and irrotational. Its governing equation is obtained from the time domain harmonic oscillation equation (eq. (1b)), where  $p$  represents the hydrodynamic pressure. After that, eq. (1b) is converted to the Helmholtz equation for frequency-domain wave vibrations.

$$\begin{cases} \frac{\partial \sigma_x}{\partial x} + \frac{\partial \tau_{xy}}{\partial y} + f_x = 0 \\ \frac{\partial \sigma_y}{\partial y} + \frac{\partial \tau_{xy}}{\partial x} + f_y = 0 \end{cases} \quad (1a) \quad \nabla^2 p - \left(\frac{1}{c}\right)^2 \frac{\partial^2 p}{\partial t^2} = 0 \quad (1b)$$

From a finite element approach, it's possible to obtain the mass ( $\mathbf{M}$ ) and stiffness ( $\mathbf{K}$ ) matrices by the shape function ( $\mathbf{N}$ ), shape function's partial derivatives ( $\mathbf{B}$ ) and constitutive ( $\mathbf{D}$ ) matrices that are employed throughout the numerical implementation proceedings. For sake of simplicity, the authors' present the straightforward element's stiffness and mass matrices. A fully theoretical explanation can be found in Sousa Jr. [10].

$$\mathbf{M}_{\mathbf{E}}^{(e)} = \int_{V_E} \mathbf{N}^T \cdot \mathbf{N} dV_E \quad (2a) \quad \mathbf{K}_{\mathbf{E}}^{(e)} = \iiint_{V_E} \mathbf{B}^T \cdot \mathbf{D} \cdot \mathbf{B} dV_E \quad (2b)$$

$$\mathbf{M}_{\mathbf{f}}^{(e)} = \int_{\Omega_f} \frac{1}{c^2} \cdot \mathbf{N}^T \cdot \mathbf{N} d\Omega_f \quad (2c) \quad \mathbf{K}_{\mathbf{f}}^{(e)} = \int_{\Omega_f} \mathbf{B}^T \cdot \mathbf{B} d\Omega_f \quad (2d)$$

### 2.2 Fluid-Structure interaction

The fluid-structure interaction ensures the multiphysics character of the navigation locks since coupling sets a compatibility relation between the degrees of freedom of each domain. In essence, the structure displacement ( $\mathbf{u}$ ) causes a pressure changing on the portions of fluid at the contact interface, and on the other hand, this pressure

modification changes the natural frequencies and mode shapes of the system. The governing equation for this interaction is shown at Fig. 2a on a unidimensional example.

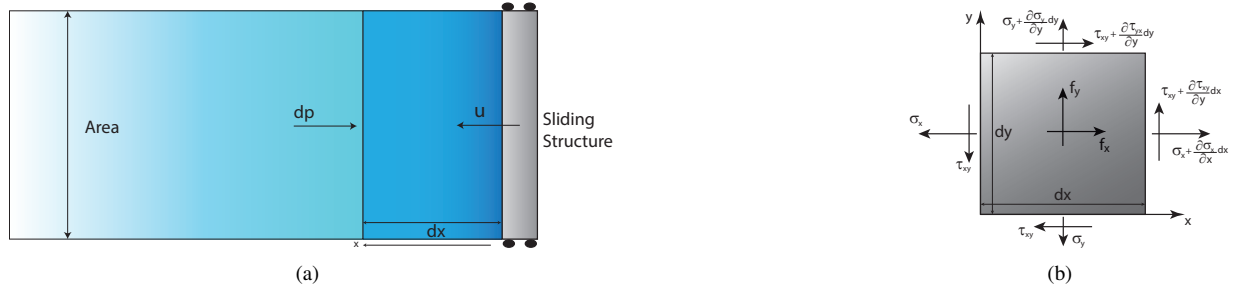


Figure 2. (a): Archetype for introducing the mechanisms of fluid-structure coupling; (b): Equilibrium of an infinitesimal element.

The fluid-structure interaction is governed by the eq. (3a) and derived from the equilibrium at  $x$  direction for a portion of fluid with specific mass ( $\rho_f$ ) near the structure's moving boundary. Its FEM formulation, given by eq. (3b), results from the shape functions  $N_p$  e  $N_u$  approximation for the pressures and displacements, respectively.

$$\vec{\nabla} p = -\rho_f \vec{\ddot{u}} \quad (3a) \quad \mathbf{FS}^T = \oint_{int} \mathbf{N}_u^T \mathbf{N}_p d\Gamma_{int} \quad (3b)$$

In doing so, the coupled problem has its final form presented by eq. (4a). The frequency domain equation (eq. (4b)) combines all degrees of freedom into the vector  $X$ , and also merges the submatrices into a general stiffness and mass matrices.

$$\begin{bmatrix} \mathbf{M}_E & \mathbf{0} \\ \rho_f \mathbf{FS} & \mathbf{M}_f \end{bmatrix} \begin{Bmatrix} \ddot{u} \\ \ddot{p} \end{Bmatrix} + \begin{bmatrix} \mathbf{K}_E & -\mathbf{FS}^T \\ \mathbf{0} & \mathbf{K}_f \end{bmatrix} \begin{Bmatrix} u \\ p \end{Bmatrix} = \mathbf{0} \quad (4a) \quad (\mathbf{K}_G - \omega^2 \mathbf{M}_G) \{X\} = \mathbf{0} \quad (4b)$$

### 2.3 Finite Element Method

The discretization of the solid domain is made by a triangular element with nodes positioned on its vertexes. Each node is ordered counter-clockwise and has two degrees of freedom -  $x$  and  $y$  displacements.

In the same fashion, fluid is treated likewise the previous domain, however, degrees of freedom are interpreted as pressures. Hence the only difference between these two elements is the reduction of two displacement degrees of freedom to a single pressure variable.

Concerning the fluid-structure coupling elements, each node combines two degrees of freedom, the first related to the structure and the second to the fluid. This element has a unidimensional geometry and nodes are located at its edges. The length for these elements is defined by the contact sides of fluid and structure domains. Given that the displacement at this interface is normal to the contour, the considered degrees of freedom for the structure are those that perform a normal displacement.

## 3 Computational Aspects

All aforementioned processes are considered on the MATLAB code developed by the authors. Even more, scripts take account of all desired operations to perform a modal analysis not only in an integrated fashion with its own auxiliary functions but also completely independent of other software. To the user are available options such as uncoupled and coupled analyses, personal inputs of geometric values, and mesh refinement.

The code is divided into three different parts. The preprocessing is responsible for the acquisition of constitutive

properties, geometric dimensions of each domain, and finally, the building of the meshes. Hereupon, the creation of stiffness and mass matrices are carried by the processor which is succeeded by the composition of the FSI matrix in the contours of the contact interface. Then global matrices are generated considering the boundary conditions for each domain when the second part terminates.

The solution of the eigenvalues, given the unsymmetrical problem at eq. (4a), is the most time-consuming task throughout the scripts, and for that matter, the native function *eigs* was used in order to obtain personalized results for the analysis. The post-processing returns values of frequency and plots the meshes.

During the implementation of this work, two strategies are present, notably: vectorization of matrices and the use of sparse matrices. Together both approaches aim to optimize the computational cost on eliminating loop structures, frequently existent in FEM codes, and as a result, they improve the time needed to conclude the analysis.

Vectorization avoids possible interaction loops used during the process of addressing elements originated from local matrices to their respective global matrices, since this strategy facilitates the indexing elements in an objective way.

Sparse matrices, as a submatrix in which most of the elements are zero, neglects zero terms that might be produced along the process. Moreover, distinct matrices with elements in the same position are properly summed, so the addressing and the final sum of each degree of freedom is made in an optimal way.

For comparison purposes, compiling and validation of the code were carried out, respectively, with MATLAB version R2019a and ANSYS Mechanical APDL 2019R3 in a computer with the following specifications: Intel Core i5-7300HQ 2.5GHz and 8GB RAM running MS Windows 10.

## 4 Numerical examples and results

Two cases are assessed by the code aforesaid. To the first case evaluated the structure cross-section is rectangular and the water depth is variable (Case I). In this way, for water depths below the crest of the dam, there are points at the wall of the structure without the inertial contribution of the fluid, and as the water depths tend to zero, values of frequency closer to an uncoupled analysis are expected.

In the second case, the structure's simplified model is completely abandoned to perform a more realistic analysis on approaching to a usual lock cross-section (Case II). The water depths variation is also present for this case due to the fact that cycles of filling and draining are frequent over the lifespan of this kind of hydraulic structure.

Dimensionless number, namely  $\alpha = H_f/H_s$ ,  $\beta = L_{cav}/L_s$ , are used along the parametric study in accordance with Fig. 3b. Case I is responsible to explore the influence of water depths variations (Fig. 3a) and different widths of the cavity (Fig. 3c).

From the Fig. 3a, it can be noticed that the presence of the fluid reduces the values of frequency of the structure starting from the fundamental frequency and becoming more prominent on higher modes. Such influence is substantiated by the effect of additional mass arose by the FSI. Still one can note that the highest water depth ( $\alpha = 1$ ) yields the maximum attenuation concerning the uncoupled case ( $\alpha = 0$ ), which happens to be the greatest contact surface that produces the utmost inertial effect caused by the fluid in the structure.

The influence of the cavity width, depicted in the Fig. 3c for  $\alpha = 1$ , is very considerable, so that when  $\beta$  values increases, smaller frequencies are experienced by the structure. That is because of the approximation towards the fluid's radiation condition at infinity, in which waves generated by the displacement of one side of the structure don't have enough energy to be reflected at the opposite wall, as a result, that reduction of frequency can act as an additional mass to the system. Besides, the curve ( $\beta^*$ ) represents the behavior of a single dam in contact with fluid on its right side. One might realize that increasing ( $\beta$ ) values yields the approximation of the lock case to the dam response.

Assessing the case of the navigation lock on its definitive shape, by the Table 1, one can verify the shifting phase behavior through the mode shapes of the system. It's possible to observe the reduction of the fundamental frequency by a quarter between the coupled and uncoupled cases, due to FSI.

## 5 Concluding Remarks

The author's proposed code represents a powerful and accessible application for modal analysis on navigation locks delivering an average error of 1% when compared with a commercial software solution, thus proving its computational accuracy. Moreover, based on the exclusive scripts, it was investigated the phenomenon of additional mass (Fig. 3a), which the highest water depth yields the greatest reductions of vibration, besides the observance of the radiation condition at infinity (Fig. 3b), in which for larger cavities, locks tend to behave as two dissociated dams ( $\beta^*$ ). Ultimately, when it comes to the problem's real geometry, (Table 1), the code exhibited versatility performing coupled and uncoupled analyses in a complex geometry with high precision, therefore justifying its relevance on

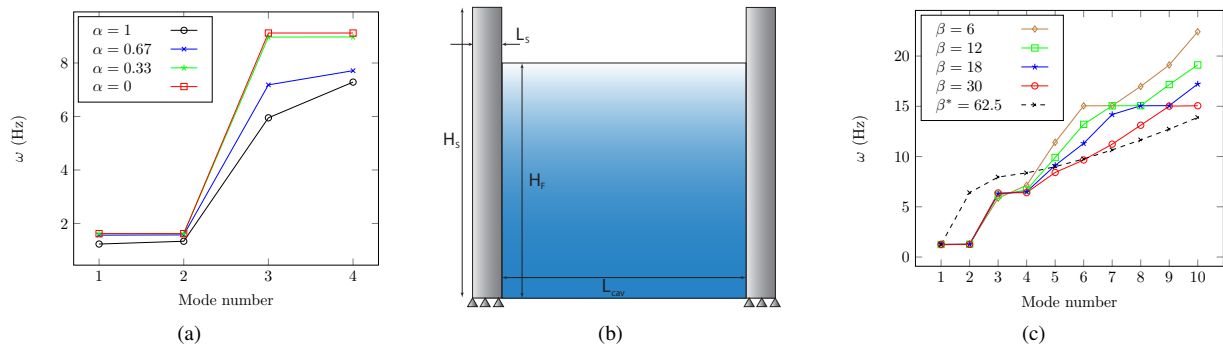


Figure 3. (a): Results for water depths variations; (b): Scheme for dimensionless consideration; (c): Results for width of the cavity variation.

Table 1. Frequency values for the case II and its mode shapes

Coupled domains					Uncoupled structure				
Frequency	ANSYS	Code	Error (%)	Modes	Frequency	ANSYS	Code	Error (%)	Modes
1	4.51	4.54	0.66		1	6.11	6.15	0.65	
2	5.34	5.39	0.93		1	6.11	6.15	0.65	
3	8.41	8.47	0.71		2	15.28	15.44	1.05	
4	13.62	13.84	1.61		2	15.28	15.44	1.05	

displaying satisfactory dynamic response values that are crucial to the design of reinforced concrete locks on considering dynamic coupling caused by the fluid-structure interaction.

**Authorship statement**

The authors hereby confirm that they are the sole liable persons responsible for the authorship of this work, and that all material that has been herein included as part of the present paper is either the property (and authorship) of the authors, or has the permission of the owners to be included here.

**References**

[1] Westergaard, H. M., 1933. Water pressures on dams during earthquakes. *ASCE*, vol. 98, pp. 418–433.  
 [2] Housner, G. W., 1963. The dynamic behavior of water tanks. *BSSA*, vol. 53, pp. 381–387.  
 [3] Reitherman, R., 2008. International aspects of the history of earthquake engineering part i. *Earthquake Engineering Research Institute*.  
 [4] Rezaiee-Pajand, 2016. Analytical solution for free vibration of flexible 2d rectangular tanks. *Ocean Engineering*, vol. 122, pp. 118–135.  
 [5] Ma, C., 2014. Dynamic behavior of flexible rectangular fluid containers with time varying fluid. *Vibroengineering*, vol. 16, pp. 3712–3725.  
 [6] Xing, J., 1997. Natural vibration of beam-water interaction system. *Sound and Vibration*, vol. 199, pp. 491–512.  
 [7] Miquel, B., 2011. Practical dynamic analysis of structures laterally vibrating in contact with water. *Computer and Structures*, vol. 89, pp. 2195–2210.  
 [8] Mendes, N. B., 2018. Um estudo de propagação de ondas e aplicação do sismo na análise dinâmica acoplada a barragem em arco.  
 [9] Transportation, 2014. Projeto de eclusas começa a ser discutido. *Jornal da Camara*, vol. 3153, pp. 7.  
 [10] Sousa Jr., L. C., 2006. Uma aplicação dos métodos dos elementos finitos e das diferenças finitas à interação fluido-estrutura.